Half-lives of α-decaying nuclei in the medium-mass region within the transfer matrix method

Shuangxiang Wu,[1] Yibin Qian,[1,2,*] and Zhongzhou Ren[3,†]

[1]*Department of Applied Physics, Nanjing University of Science and Technology, Nanjing 210094, China*

[2]*Department of Physics, KTH Royal Institute of Technology, 10691 Stockholm, Sweden*

[3]*School of Physics Science and Engineering, Tongji University, Shanghai 200092, China*

(Received 30 January 2018; published 15 May 2018)

The α-decay half-lives of even-even nuclei from Sm to Th are systematically studied based on the transfer matrix method. For the nuclear potential, a type of cosh-parametrized form is applied to calculate the penetration probability. Through a least-squares fit to experimental half-lives, we optimize the parameters in the potential and the α preformation factor P_0. During this process, P_0 is treated as a constant for each parent nucleus. Eventually, the calculated half-lives are found to agree well with the experimental data, which verifies the accuracy of the present approach. Furthermore, in recent studies, P_0 is regulated by the shell and paring effects plus the nuclear deformation. To this end, P_0 is here associated with the structural quantity, i.e., the microscopic correction of nuclear mass ($E_{\rm mic}$). In this way, the agreement between theory and experiment is greatly improved by more than 20%, validating the appropriate treatment of P_0 in the scheme of $E_{\rm mic}$.

DOI: 10.1103/PhysRevC.97.054316

I. INTRODUCTION

In 1899, α particles were first defined in the investigations of radioactivity by Ernest Rutherford, in an early development of nuclear physics. Since then, α emission has been known as an important decay channel of unstable nuclei, and has provided much reliable information on nuclear structure such as ground-state energy, nuclear spin plus parity, and nuclear deformation [1–3]. Especially, measurements on the α-decay chain are used as the main tool to identify new superheavy elements or isotopes [4–12], and the α-decay spectrum is considered an effective way to detect the structure properties of neutron-deficient nuclei as well [2,13]. Therefore, renewed interest has been stimulated for experimental and theoretical research on α decay.

In the 1920s, Gamow successfully explained the theory of α-decay process as a quantum tunneling effect, which can be taken as the first application of quantum mechanics in nuclear physics [14]. The α decay can be described as two independent processes, namely the formation of an α particle at the surface of the parent nucleus, and the sequential barrier tunneling [15,16]. Extensive studies have been devoted to this decay mode and to heavier cluster emissions based on various models [17–40], such as a cluster model [21–23], the generalized liquid drop model (GLDM) [24,25], the density-dependent M3Y interaction and the mean-field potential [26–33], and the analytical superasymmetric fission (ASAF) model [34–40]. Besides, many phenomenological formulas, including several structural ingredients, have been proposed to evaluate the half-lives of α and cluster emitters as well [34,41–48]. In these calculations, the experimental α-decay half-lives can be generally reproduced with a factor of 3–4. At present, we choose a widely used type of cosh-parameterized form to calculate the penetration probability. Then, the most difficult part is how to estimate the α-preformation probability P_0 that the α particle exists as a recognizable entity inside the nucleus before its emission. On one hand, due to the complexity of nuclear many-body problem and nuclear potential, it is extremely difficult to perform a microscopic description for the preformation factor P_0. On the other hand, P_0 appears to vary smoothly in the open-shell region according to a detailed analysis of experimental facts [1]. With these in mind, P_0 is taken as a constant for one kind of nuclei to precede the whole calculation of α-decay half-lives [21–23,31]. However, based on recent studies [2,49–52], the pairing and shell effects should play an important role in the formation of the emitted α particle. As an alternative, P_0 may be connected with a structure quantity, i.e., microscopic correction of nuclear mass ($E_{\rm mic}$), which takes into account these aforementioned influences to a great extent.

In this work, to explain the tunneling process, we adopt the transfer matrix method to calculate the penetration probability instead of the well-known Wentzel-Kramers-Brillouin (WKB) semiclassical approximation. The transfer matrix method has been employed in the research of semiconductor physics and even nuclear reactions, as in the calculation of transmission tunneling current [53] and the fusion cross section [54]. But up to now, it seems that this method is not that commonly applied in the investigation of α decay, in particular for systematic calculations. Hence, we here propose to introduce this approach into α-decay studies, not only aiming at checking its accuracy for calculating α-decay half-lives, but also providing a different perspective.

This paper is organized as follows. In Sec. II, a brief introduction of the transfer matrix method is given first, and the α-core potential is then presented in a specific form. In

*qyibin@njust.edu.cn

†zren@tongji.edu.cn, zren@nju.edu.cn

addition, two different methods are offered to obtain the α preformation factor P_0. The numerical results are shown and discussed in Sec. III. In the last section, we draw conclusions and propose future work.

II. THEORETICAL FRAMEWORK

A. Transfer matrix method

To calculate the penetration probability across an arbitrary potential barrier of a particle, we can always split the potential barrier into N segments, in which the potential energy can be treated as a constant. Then the potential barrier $V(r)$ and the effective mass $m^*(r)$ are approximated by the multistep functions (see details in Ref. [53] and references therein)

$$V(r) = V_j = V[(r_{j-1} + r_j)/2], \tag{1}$$

$$m^*(r) = m^*_j = m^*[(r_{j-1} + r_j)/2] \tag{2}$$

for $r_{j-1} < r < r_j$ $(j = 0,1,\ldots,N,N+1)$.

The wave function $\psi_j(r)$ in the jth region, corresponding to a particle with energy E, can be expressed as

$$\psi_j(r) = A_j \exp(ik_j r) + B_j \exp(-ik_j r), \tag{3}$$

where

$$k_j = \sqrt{2m^*_j(E - V_j)}/\hbar. \tag{4}$$

From the continuity of the wave function and its derivative at each boundary, the determination of A_j and B_j in Eq. (3) can be reduced to the multiplication of the following $N+1$ (2×2) matrices:

$$\begin{pmatrix} A_j \\ B_j \end{pmatrix} = \prod_{l=0}^{j-1} M_l \begin{pmatrix} A_0 \\ B_0 \end{pmatrix}, \tag{5}$$

where

$$M_l = \frac{1}{2}\begin{pmatrix} (1+S_l)\exp[-i(k_{l+1}-k_l)r_l] & (1-S_l)\exp[-i(k_{l+1}+k_l)r_l] \\ (1-S_l)\exp[i(k_{l+1}+k_l)r_l] & (1+S_l)\exp[i(k_{l+1}-k_l)r_l] \end{pmatrix}, \tag{6}$$

and

$$S_l = \frac{m^*_{l+1}}{m^*_l}\frac{k_l}{k_{l+1}}. \tag{7}$$

By setting $A_0 = 1$ and $B_{N+1} = 0$ in Eq. (3) for $j = N+1$, we can calculate the transmission amplitude A_{N+1} and the penetration probability $T(E)$ as follows:

$$A_{N+1} = \frac{m^*_0}{m^*_{N+1}}\frac{k_0}{k_{N+1}}\frac{1}{M_{22}}, \tag{8}$$

$$T(E) = \frac{m^*_0}{m^*_{N+1}}\frac{k_{N+1}}{k_0}|A_{N+1}|^2, \tag{9}$$

where

$$M = \begin{pmatrix} M_{11} & M_{12} \\ M_{21} & M_{22} \end{pmatrix} = \prod_{l=0}^{N} M_l. \tag{10}$$

B. Parameters in α-core potential and the α preformation factor

The α-decay half-life is determined by the decay constant λ. It can be expressed as follows:

$$T_{1/2} = \frac{\ln 2}{\lambda}, \tag{11}$$

where the decay constant is defined as

$$\lambda = P_0 \nu_0 P. \tag{12}$$

Here the penetration probability P is obtained by Eq. (9), and P_0 denotes the preformation probability of α cluster before its emission. For the assault frequency, imagine that the α particle moves back and forth inside the nucleus with a velocity $v = \sqrt{\frac{2E_\alpha}{M}}$; then it presents itself at the barrier with a frequency

$$\nu_0 = \left(\frac{1}{2R}\sqrt{\frac{2E_\alpha}{M}}\right). \tag{13}$$

E_α is the kinetic energy of α particle, which has been corrected for recoil, and M is the mass of the α particle. and R is the radius of the parent nucleus expressed by an empirical formula [24,25],

$$R = (1.28A^{1/3} - 0.76 + 0.8A^{-1/3})\ \text{fm}. \tag{14}$$

Undoubtedly, the α-core potential is crucial to obtain the penetration probability P via the transfer matrix method. It is composed of nuclear, Coulomb, and centrifugal terms, namely

$$V(r) = V_N(r) + V_C(r) + V_l(r). \tag{15}$$

For the nuclear potential $V_N(r)$, we choose a widely used type of cosh-parametrized form:

$$V_N(r) = -\frac{V_0[1+\cosh(R/a)]}{\cosh(r/a) + \cosh(R/a)}, \tag{16}$$

where the parameters V_0 and a denote the depth and diffuseness of the potential, respectively. The Coulomb potential $V_C(r)$ is taken as the form of a point α cluster interacting with a uniformly charged sphere of radius R,

$$V_C(r) = \begin{cases} \frac{Z_d Z_\alpha e^2}{2R}\left[3 - \left(\frac{r}{R}\right)^2\right], & r \leqslant R, \\ \frac{Z_d Z_\alpha e^2}{r}, & r > R, \end{cases} \tag{17}$$

where Z_d and Z_α are separately the proton numbers of the daughter nucleus and the α particle. The centrifugal potential $V_l(r)$ is usually expressed as $V_l(r) = \frac{l(l+1)\hbar^2}{2\mu r^2}$, where l is the orbital angular momentum of the α particle. Actually, in the α

decay for even-even nuclei, the angular momentum l usually equals zero [25], leading to $V_l(r) = 0$.

As mentioned before, the preformation factor P_0 [in Eq. (12)] is very difficult to describe in a fully microscopical way due to the complexity of the nuclear many-body problem. Experimentally, P_0 is found to vary smoothly in the open-shell region and has a value no more than 1.0 [1]. In this sense, it is reasonable and appropriate to treat P_0 as a constant for one kind of nuclei. We adopt this treatment in the first case of our calculation, which is denoted by "Cal.1". Specifically, the parameters V_0 and a in Eq. (16) and P_0 are totally determined by a least-squares fit to the experimental half-lives; the calculated half-lives can then in turn be obtained for all studied nuclei. On the other hand, considering that the pairing and shell effects play a significant role in the formation process of the emitted α particle [2,49–52], we propose to connect the preformation factor P_0 with related structural quantities. According to our systematic analysis (which can be seen in the following section), the preformation factor is supposed to behave in the following pattern:

$$\log_{10} P_0 = c_1 E_{\rm mic} + c_2, \tag{18}$$

where $E_{\rm mic}$ is the microscopic correction of nuclear mass [55], corresponding to the influence of pairing and shell plus nuclear deformation. Similarly, all the parameters, V_0 and a in the potential plus c_1 and c_2 in Eq. (18), are completely optimized to match the experimental α-decay half-lives, through the aforementioned calculating procedure (indicated by "Cal.2").

III. RESULTS AND DISCUSSIONS

Within the above framework, we have systematically calculated the α-decay half-lives for even-even medium nuclei with $82 < N < 126$. In the case of Cal.1, the critical parameters are determined as follows:

$$\begin{aligned} V_0 &= 170.00 \text{ MeV}, \\ a &= 0.7668 \text{ fm}, \\ P_0 &= 0.21. \end{aligned} \tag{19}$$

Accordingly, the root mean square (rms) deviation, $\Delta = \sqrt{\frac{1}{n}\sum_{i=1}^{n}(\log_{10} T_{1/2}^{{\rm cal}\ i} - \log_{10} T_{1/2}^{{\rm exp}\ i})^2}$, is 0.292, which indicates that the present approach is reasonable and valid to investigate the α-decay process. To gain a deep view, we have also plotted the deviation between calculation and experiment versus the neutron number of each parent nucleus in Fig. 1. As one can see, the majority of the $\log_{10}(T_{1/2}^{\rm cal}/T_{1/2}^{\rm exp})$ values are located between -0.5 and 0.5. This means the experimental α-decay half-lives are well reproduced within the range of about 0.3 to 3. Furthermore, the absolute values of $\log_{10}(T_{1/2}^{\rm cal}/T_{1/2}^{\rm exp})$ have a visible tendency to increase as neutron number N reaches the spherical shell closures $N = 82$ and $N = 126$, reconfirming the shell effects on α decay [2,50].

Based on the results of Cal.1 along the potential parameters V_0 and a of Eq. (19), we can in fact extract the preformation factor via the ratio of the experimental decay constant to the calculated one. In order to check our previous conjecture on P_0, namely Eq. (18), we plot the deduced $\log_{10} P_0$ versus

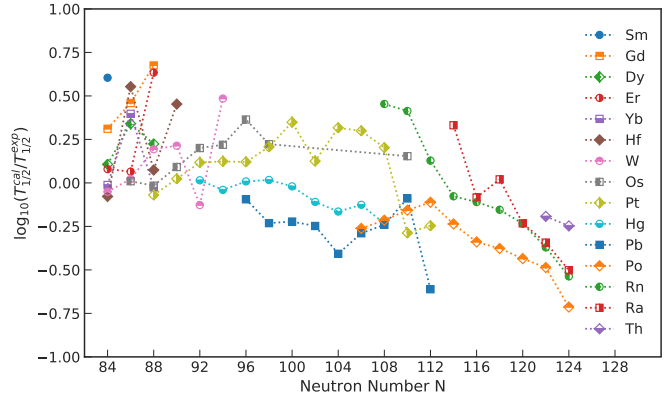

FIG. 1. The logarithmic deviations between calculated half-lives and experimental data versus the neutron number N of the parent nucleus for various isotopic chains. Note that all the calculated half-lives are obtained in the case of Cal.1.

the microscopic correction of nuclear mass $E_{\rm mic}$ (in MeV) [55] in Fig. 2. As clearly shown, there is generally a linear relationship between $\log_{10} P_0$ and $E_{\rm mic}$, which supports our previous speculation. In turn, as mentioned previously, it is reasonable to depict P_0 by Eq. (18). On the basis of our optimization, the parameters V_0 and a in the potential barrier are finally determined as follows:

$$\begin{aligned} V_0 &= 170.11 \text{ MeV}, \\ a &= 0.7672 \text{ fm}. \end{aligned} \tag{20}$$

Meanwhile, the parameters in Eq. (18) are fixed as $c_1 = 0.086$, $c_2 = -0.62$. Correspondingly, the rms deviation between $\log_{10} T_{1/2}^{\rm cal}$ and $\log_{10} T_{1/2}^{\rm exp}$ drops to 0.217, implying that the results of Cal.2 are improved by $\frac{0.292-0.217}{0.292}\% = 25.7\%$. To present a better insight, the $\log_{10}(T_{1/2}^{\rm cal}/T_{1/2}^{\rm exp})$ (Cal.2) has been graphed for various isotopes in Fig. 3. One can see that the absolute deviations generally incline to the zero point as compared to the situation in Fig. 1, denoting an obvious improvement of calculation accuracy. In particular, the large discrepancies between $T_{1/2}^{\rm cal}$ and $T_{1/2}^{\rm exp}$ decrease apparently when

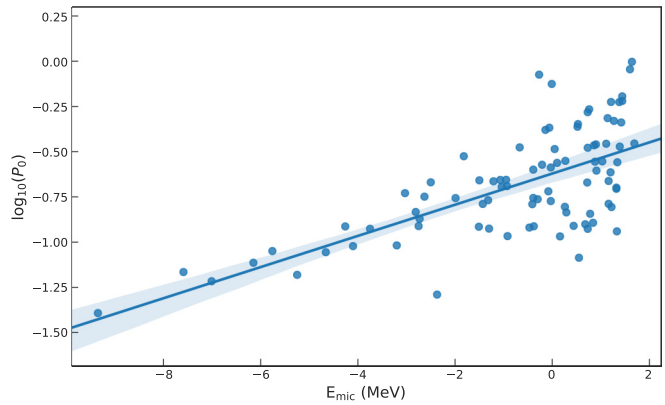

FIG. 2. Extracted P_0 (in logarithmic scale) versus the microscopic correction (in MeV) of nuclear mass. The fitted line with the error shadow is added to guide the eye.

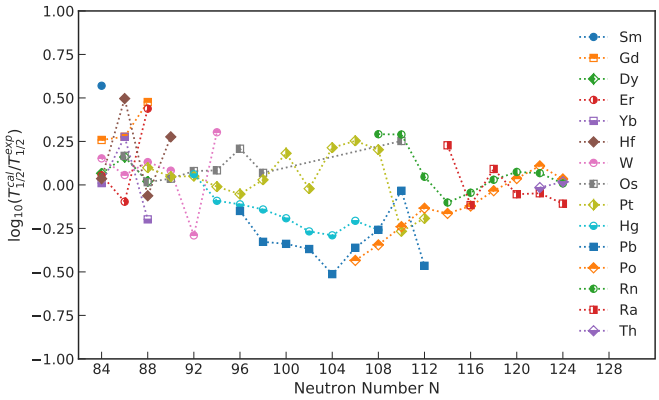

FIG. 3. Same as Fig. 1, but for the case of Cal.2.

the neutron number of parent nuclei approaches the $N = 126$ shell closure, as compared to the picture of Cal.1. Therefore, one can conclude that it is indeed feasible to consider the α preformation factor in terms of the structural quantity $E_{\rm mic}$. Before the detailed analysis of this point, it is interesting to note that the deviation seems to increase when N reaches 104. As is well known, $N = 104$ is the medium number of neutron shell closures $N = 82$ and $N = 126$, indicating that those nuclei around this region carry a bunch of valence neutrons. In this sense, the corresponding configuration spaces are quite complicated, which may imply that the present treatment of P_0 in the $E_{\rm mic}$ scheme needs further consideration.

In Fig. 4, we give the absolute values $\log_{10}(T^{\rm cal}_{1/2}/T^{\rm exp}_{1/2})$ with different elements as the neutron number N achieves the spherical shell closures, i.e., $N = 84$ and $N = 124$. The absolute values are employed to directly present the differences between calculation and experiment. As clearly shown in Fig. 4, the calculated α-decay half-lives from Cal.2 are mostly improved in contrast with those from Cal.1. Especially, the absolute values $\log_{10}(T^{\rm cal}_{1/2}/T^{\rm exp}_{1/2})$ of Cal.2 are much smaller for the $N = 124$ isotones, further supporting that the treatment, associating P_0 with $E_{\rm mic}$, takes into account the shell effects on α preformation to a great extent. Besides the isotones, we also provide the comparison of two typical isotopic chains from another viewpoint in Fig. 5. Specifically, we present the $|\log_{10}(T^{\rm cal}_{1/2}/T^{\rm exp}_{1/2})|$ values via different P_0 treatments (Cal.1 and Cal.2) for the isotopes of elements Po and Rn. As can be

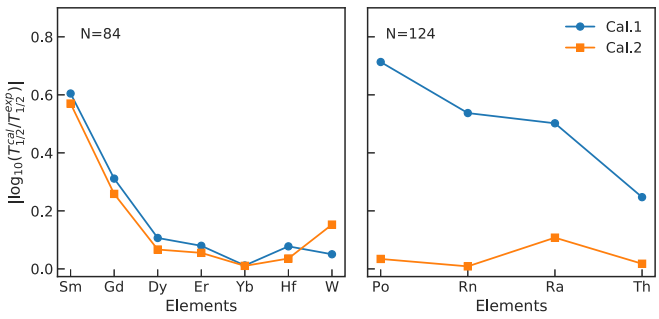

FIG. 4. The absolute $\log_{10}(T^{\rm cal}_{1/2}/T^{\rm exp}_{1/2})$ values versus different elements for the $N = 84$ and $N = 124$ isotonic chains. The circles and squares represent the results from Cal.1 and Cal.2, respectively.

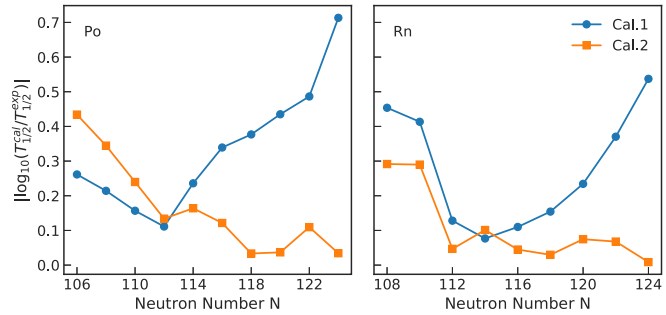

FIG. 5. The absolute $\log_{10}(T^{\rm cal}_{1/2}/T^{\rm exp}_{1/2})$ values versus the neutron number N of the parent nucleus for the isotopic chains of elements Po and Rn. The solid circles and squares represent the results using Cal.1 and Cal.2, respectively.

seen, almost all the deviations obtained by Cal.2 are below those points of Cal.1. More interestingly, one can see that the difference between calculated results of Cal.1 and Cal.2 appears to be relatively small when the parent nucleus is

TABLE I. Comparisons of our calculated half-lives with the experimental data for even-even nuclei with neutron number $82 < N < 126$.

Element	A	Q_α (MeV)	$T^{\rm exp}_{1/2}$ (s)	$T^{\rm Cal.1}_{1/2}$ (s)	$T^{\rm Cal.2}_{1/2}$ (s)
Sm	146	2.529	2.14×10^{15}	8.62×10^{15}	7.96×10^{15}
Gd	148	3.271	2.23×10^{9}	4.57×10^{9}	4.05×10^{9}
	150	2.807	5.64×10^{13}	1.62×10^{14}	1.06×10^{14}
	152	2.204	3.41×10^{21}	1.61×10^{22}	1.02×10^{22}
Dy	150	4.351	1.20×10^{3}	1.53×10^{3}	1.39×10^{3}
	152	3.727	8.57×10^{6}	1.87×10^{7}	1.23×10^{7}
	154	2.945	9.46×10^{13}	1.58×10^{14}	9.92×10^{13}
Er	152	4.934	1.14×10^{1}	1.36×10^{1}	1.29×10^{1}
	154	4.280	4.76×10^{4}	5.52×10^{4}	3.81×10^{4}
	156	3.487	6.88×10^{9}	2.96×10^{10}	1.88×10^{10}
Yb	154	5.474	4.41×10^{-1}	4.29×10^{-1}	4.51×10^{-1}
	156	4.810	2.61×10^{2}	6.51×10^{2}	4.93×10^{2}
	158	4.170	4.26×10^{6}	4.00×10^{6}	2.70×10^{6}
Hf	156	6.029	2.37×10^{-2}	1.98×10^{-2}	2.57×10^{-2}
	158	5.405	2.23×10^{0}	7.97×10^{0}	6.99×10^{0}
	160	4.902	1.94×10^{3}	2.30×10^{3}	1.68×10^{3}
	162	4.416	4.94×10^{5}	1.40×10^{6}	9.33×10^{5}
W	158	6.613	1.25×10^{-3}	1.11×10^{-3}	1.77×10^{-3}
	160	6.066	1.03×10^{-1}	1.08×10^{-1}	1.17×10^{-1}
	162	5.678	2.63×10^{0}	4.10×10^{0}	3.55×10^{0}
	164	5.278	1.66×10^{2}	2.71×10^{2}	2.00×10^{2}
	166	4.856	5.49×10^{4}	4.09×10^{4}	2.81×10^{4}
	168	4.500	1.59×10^{6}	4.85×10^{6}	3.19×10^{6}
Os	162	6.767	2.10×10^{-3}	2.14×10^{-3}	3.08×10^{-3}
	164	6.479	2.14×10^{-2}	2.06×10^{-2}	2.22×10^{-2}
	166	6.143	2.96×10^{-1}	3.65×10^{-1}	3.21×10^{-1}
	168	5.816	4.88×10^{0}	7.74×10^{0}	5.86×10^{0}
	170	5.537	7.76×10^{1}	1.28×10^{2}	9.40×10^{1}
	172	5.224	1.75×10^{3}	4.04×10^{3}	2.82×10^{3}
	174	4.871	1.83×10^{5}	3.05×10^{5}	2.14×10^{5}
	186	2.821	6.31×10^{22}	8.99×10^{22}	1.12×10^{23}

TABLE I. (*Continued.*)

Element	A	Q_α (MeV)	$T_{1/2}^{\rm exp}$ (s)	$T_{1/2}^{\rm Cal.1}$ (s)	$T_{1/2}^{\rm Cal.2}$ (s)
Pt	166	7.286	3.00×10^{-4}	2.55×10^{-4}	3.76×10^{-4}
	168	6.990	2.02×10^{-3}	2.13×10^{-3}	2.25×10^{-3}
	170	6.707	1.42×10^{-2}	1.86×10^{-2}	1.59×10^{-2}
	172	6.463	1.01×10^{-1}	1.34×10^{-1}	9.86×10^{-2}
	174	6.183	1.17×10^{0}	1.54×10^{0}	1.03×10^{0}
	176	5.885	1.59×10^{1}	2.56×10^{1}	1.70×10^{1}
	178	5.573	2.83×10^{2}	6.32×10^{2}	4.29×10^{2}
	180	5.240	2.03×10^{4}	2.70×10^{4}	1.93×10^{4}
	182	4.951	4.63×10^{5}	9.60×10^{5}	7.57×10^{5}
	184	4.599	6.10×10^{7}	1.21×10^{8}	1.09×10^{8}
	186	4.320	5.35×10^{9}	8.53×10^{9}	8.52×10^{9}
	188	4.007	3.39×10^{12}	1.74×10^{12}	1.83×10^{12}
	190	3.269	2.05×10^{19}	1.16×10^{19}	1.31×10^{19}
Hg	172	7.524	2.31×10^{-4}	2.39×10^{-4}	2.66×10^{-4}
	174	7.233	2.00×10^{-3}	1.82×10^{-3}	1.62×10^{-3}
	176	6.897	2.26×10^{-2}	2.30×10^{-2}	1.74×10^{-2}
	178	6.577	2.99×10^{-1}	3.10×10^{-1}	2.16×10^{-1}
	180	6.258	5.39×10^{0}	5.15×10^{0}	3.47×10^{0}
	182	5.996	7.85×10^{1}	6.10×10^{1}	4.24×10^{1}
	184	5.662	2.78×10^{3}	1.90×10^{3}	1.42×10^{3}
	186	5.204	5.17×10^{5}	3.87×10^{5}	3.21×10^{5}
	188	4.707	5.27×10^{8}	3.07×10^{8}	2.90×10^{8}
Pb	178	7.790	2.30×10^{-4}	1.85×10^{-4}	1.63×10^{-4}
	180	7.419	4.10×10^{-3}	2.40×10^{-3}	1.93×10^{-3}
	182	7.066	5.61×10^{-2}	3.36×10^{-2}	2.57×10^{-2}
	184	6.774	6.12×10^{-1}	3.46×10^{-1}	2.62×10^{-1}
	186	6.470	1.20×10^{1}	4.72×10^{0}	3.70×10^{0}
	188	6.109	2.73×10^{2}	1.40×10^{2}	1.18×10^{2}
	190	5.698	1.77×10^{4}	1.02×10^{4}	9.79×10^{3}
	192	5.221	3.56×10^{6}	2.89×10^{6}	3.29×10^{6}
	194	4.738	8.79×10^{9}	2.15×10^{9}	3.01×10^{9}
Po	190	7.693	2.46×10^{-3}	1.34×10^{-3}	9.05×10^{-4}
	192	7.320	3.31×10^{-2}	2.02×10^{-2}	1.49×10^{-2}
	194	6.987	3.92×10^{-1}	2.73×10^{-1}	2.25×10^{-1}
	196	6.658	5.67×10^{0}	4.38×10^{0}	4.16×10^{0}
	198	6.310	1.85×10^{2}	1.07×10^{2}	1.26×10^{2}
	200	5.982	6.22×10^{3}	2.84×10^{3}	4.70×10^{3}
	202	5.701	1.39×10^{5}	5.85×10^{4}	1.29×10^{5}
	204	5.485	1.89×10^{6}	6.94×10^{5}	2.05×10^{6}
	206	5.327	1.39×10^{7}	4.55×10^{6}	1.79×10^{7}
	208	5.215	9.14×10^{7}	1.76×10^{7}	9.89×10^{7}
Rn	194	7.862	7.80×10^{-4}	2.21×10^{-3}	1.52×10^{-3}
	196	7.617	4.70×10^{-3}	1.21×10^{-2}	9.16×10^{-3}
	198	7.349	6.56×10^{-2}	8.82×10^{-2}	7.31×10^{-2}
	200	7.043	1.18×10^{0}	9.93×10^{-1}	9.38×10^{-1}
	202	6.774	1.24×10^{1}	9.62×10^{0}	1.11×10^{1}
	204	6.547	1.03×10^{2}	7.22×10^{1}	1.10×10^{2}
	206	6.384	5.49×10^{2}	3.20×10^{2}	6.52×10^{2}
	208	6.261	2.35×10^{3}	1.00×10^{3}	2.75×10^{3}
	210	6.159	9.00×10^{3}	2.61×10^{3}	9.18×10^{3}
Ra	202	7.880	4.10×10^{-3}	8.79×10^{-3}	6.92×10^{-3}
	204	7.637	6.00×10^{-2}	4.94×10^{-2}	4.59×10^{-2}
	206	7.415	2.46×10^{-1}	2.57×10^{-1}	3.03×10^{-1}
	208	7.273	1.27×10^{0}	7.47×10^{-1}	1.12×10^{0}
	210	7.151	4.17×10^{0}	1.89×10^{0}	3.73×10^{0}
	212	7.032	1.53×10^{1}	4.82×10^{0}	1.19×10^{1}
Th	212	7.958	3.17×10^{-2}	2.03×10^{-2}	3.06×10^{-2}
	214	7.827	8.70×10^{-2}	4.92×10^{-2}	9.06×10^{-2}

located in the medium region of two major shell closures, like $N = 106$–112. This fact somewhat supports the mentioned smooth behavior of the α preformation factor in the open shell region. In addition, the detailed numerical results of the α-decay half-lives for even-even nuclei with neutron number $82 < N < 126$ are listed in Table I. The first and second columns give the element and the mass number of the parent nucleus, respectively. The third and forth columns correspond to the experimental decay energy and half-lives [56–58], and the half-lives calculated by methods Cal.1 and Cal.2 are presented in the last two columns, respectively. In general, the transfer matrix method can be applied to the large-range calculation of α-decay half-lives, and it is a possible way to obtain the preformation factor P_0 with the help of the microscopic correction of nuclear mass.

IV. SUMMARY

In summary, the half-lives of α-decaying nuclei with $82 < N < 126$ have been calculated with the transfer matrix method, where the α-core potential is described by the parametrized form of cosh terms. Then, we adopt two different strategies to obtain the α preformation factor P_0, namely a constant treatment (Cal.1) and the relationship with $E_{\rm mic}$ (Cal.2). No matter which one is considered, the final results are found to agree well with the experimental data. In detail, the standard deviation between theory and experiment in Cal.2 is reduced by more than 20% as compared to that in Cal.1, which confirms the effectiveness of the relationship between the α preformation factor and the structural quantity $E_{\rm mic}$. In the meantime, the effects of the $N = 82$ and $N = 126$ shell closures are reconfirmed for α-decay processes via comparative analysis of various isotopes, further demonstrating the rationality of associating P_0 with $E_{\rm mic}$. Encouraged by the obviously enhanced accuracy of the results in Cal.2, it is hoped that the present study can be extended to other regions of neutron-deficient isotopes, especially superheavy elements.

ACKNOWLEDGMENTS

The author Y.Q. thanks C. Qi for the careful reading and suggestions. This work is supported by the National Natural Science Foundation of China (Grants No. 11375086, No. 11535004, No. 11605089, and No. 11120101005), by the Natural Science Youth Fund of Jiangsu Province (Grant No. BK20150762), by the Fundamental Research Funds for the Central Universities (Grant No. 30916011339), and by the National Major State Basic Research and Development Program of China (Grant No. 2016YFE0129300). Y.Q. is supported in part by the China Scholarship Council (CSC) (Grant No. 201700260234).

[1] P. E. Hodgson and E. Běták, Phys. Rep. **374**, 1 (2003).

[2] A. N. Andreyev, M. Huyse, P. Van Duppen, C. Qi, R. J. Liotta, S. Antalic, D. Ackermann, S. Franchoo, F. P. Heßberger, S. Hofmann, I. Kojouharov, B. Kindler, P. Kuusiniemi, S. R. Lesher, B. Lommel, R. Mann, K. Nishio, R. D. Page, B. Streicher, Š. Šáro, B. Sulignano, D. Wiseman, and R. A. Wyss, Phys. Rev. Lett. **110**, 242502 (2013).

[3] Z. Ren and G. Xu, Phys. Rev. C **36**, 456 (1987).

[4] S. Hofmann and G. Münzenberg, Rev. Mod. Phys. **72**, 733 (2000).

[5] Yu. Ts. Oganessian, F. Sh. Abdullin, C. Alexander, J. Binder, R. A. Boll, S. N. Dmitriev, J. Ezold, K. Felker, J. M. Gostic, R. K. Grzywacz, J. H. Hamilton, R. A. Henderson, M. G. Itkis, K. Miernik, D. Miller, K. J. Moody, A. N. Polyakov, A. V. Ramayya, J. B. Roberto, M. A. Ryabinin, K. P. Rykaczewski, R. N. Sagaidak, D. A. Shaughnessy, I. V. Shirokovsky, M. V. Shumeiko, M. A. Stoyer, N. J. Stoyer, V. G. Subbotin, A. M. Sukhov, Y. S. Tsyganov, V. K. Utyonkov, A. A. Voinov, and G. K. Vostokin, Phys. Rev. Lett. **109**, 162501 (2012).

[6] Yu. Ts. Oganessian and V. K. Utyonkov, Rep. Prog. Phys. **78**, 036301 (2015).

[7] K. Morita, K. Morimoto, D. Kaji, H. Haba, K. Ozeki, Y. Kudou, T. Sumita, Y. Wakabayashi, A. Yoneda, K. Tanaka, S. Yamaki, R. Sakai, T. Akiyama, S.-i. Goto, H. Hasebe, M. Huang, T. Huang, E. Ideguchi, Y. Kasamatsu, K. Katori, Y. Kariya, H. Kikunaga, H. Koura, H. Kudo, A. Mashiko, K. Mayama, S.-i. Mitsuoka, T. Moriya, M. Murakami, H. Murayama, S. Namai, A. Ozawa, N. Sato, K. Sueki, M. Takeyama, F. Tokanai, T. Yamaguchi, and A. Yoshida, J. Phys. Soc. Jpn. **81**, 103201 (2012).

[8] Ch. E. Düllmann, M. Schädel, A. Yakushev, A. Türler, K. Eberhardt, J. V. Kratz, D. Ackermann, L.-L. Andersson, M. Block, W. Brüchle, J. Dvorak, H. G. Essel, P. A. Ellison, J. Even, J. M. Gates, A. Gorshkov, R. Graeger, K. E. Gregorich, W. Hartmann, R.-D. Herzberg, F. P. Heßberger, D. Hild, A. Hübner, E. Jäger, J. Khuyagbaatar, B. Kindler, J. Krier, N. Kurz, S. Lahiri, D. Liebe, B. Lommel, M. Maiti, H. Nitsche, J. P. Omtvedt, E. Parr, D. Rudolph, J. Runke, B. Schausten, E. Schimpf, A. Semchenkov, J. Steiner, P. Thörle-Pospiech, J. Uusitalo, M. Wegrzecki, and N. Wiehl, Phys. Rev. Lett. **104**, 252701 (2010).

[9] J. Khuyagbaatar, A. Yakushev, C. Düllmann, D. Ackermann, L.-L. Andersson, M. Asai, M. Block, R. Boll, H. Brand, D. Cox, M. Dasgupta, X. Derkx, A. Di Nitto, K. Eberhardt, J. Even, M. Evers, C. Fahlander, U. Forsberg, J. Gates, N. Gharibyan, P. Golubev, K. Gregorich, J. Hamilton, W. Hartmann, R.-D. Herzberg, F. Heßberger, D. Hinde, J. Hoffmann, R. Hollinger, A. Hübner, E. Jäger, B. Kindler, J. Kratz, J. Krier, N. Kurz, M. Laatiaoui, S. Lahiri, R. Lang, B. Lommel, M. Maiti, K. Miernik, S. Minami, A. Mistry, C. Mokry, H. Nitsche, J. Omtvedt, G. Pang, P. Papadakis, D. Renisch, J. Roberto, D. Rudolph, J. Runke, K. Rykaczewski, L. Sarmiento, M. Schädel, B. Schausten, A. Semchenkov, D. Shaughnessy, P. Steinegger, J. Steiner, E. Tereshatov, P. Thörle-Pospiech, K. Tinschert, T. Torres De Hei-denreich, N. Trautmann, A. Türler, J. Uusitalo, D. Ward, M. Wegrzecki, N. Wiehl, S. Van Cleve, and V. Yakusheva, Phys. Rev. Lett. **112**, 172501 (2014).

[10] S. Hofmann, J. Phys. G: Nucl. Part. Phys. **42**, 114001 (2015).

[11] P. A. Ellison, K. E. Gregorich, J. S. Berryman, D. L. Bleuel, R. M. Clark, I. Dragojević, J. Dvorak, P. Fallon, C. Fineman-Sotomayor, J. M. Gates, O. R. Gothe, I. Y. Lee, W. D. Loveland, J. P. McLaughlin, S. Paschalis, M. Petri, J. Qian, L. Stavsetra, M. Wiedeking, and H. Nitsche, Phys. Rev. Lett. **105**, 182701 (2010).

[12] L. Stavsetra, K. E. Gregorich, J. Dvorak, P. A. Ellison, I. Dragojević, M. A. Garcia, and H. Nitsche, Phys. Rev. Lett. **103**, 132502 (2009).

[13] C. Qi, Rev. Phys. **1**, 77 (2016).

[14] G. Gamow, Z. Phy. **51**, 204 (1928).

[15] D. N. Poenaru and W. Greiner, *Handbook of Nuclear Properties* (Clarendon, Oxford, 1996).

[16] D. N. Poenaru, *Nuclear Decay Modes* (Institute of Physics, Bristol, 1996).

[17] V. Yu. Denisov, O. I. Davidovskaya, and I. Y. Sedykh, Phys. Rev. C **92**, 014602 (2015).

[18] D. N. Poenaru, R. A. Gherghescu, and W. Greiner, Phys. Rev. C **83**, 014601 (2011).

[19] K. P. Santhosh, J. G. Joseph, and S. Sahadevan, Phys. Rev. C **82**, 064605 (2010).

[20] Y. Ren and Z. Ren, Phys. Rev. C **85**, 044608 (2012).

[21] B. Buck, A. C. Merchant, and S. M. Perez, Phys. Rev. Lett. **65**, 2975 (1990).

[22] C. Xu and Z. Ren, Phys. Rev. C **73**, 041301 (2006).

[23] C. Xu and Z. Ren, Phys. Rev. C **74**, 014304 (2006).

[24] G. Royer and H. F. Zhang, Phys. Rev. C **77**, 037602 (2008).

[25] S. Guo, X. Bao, Y. Gao, J. Li, and H. Zhang, Nucl. Phys. A **934**, 110 (2015).

[26] P. Mohr, Phys. Rev. C **61**, 045802 (2000).

[27] P. Mohr, Phys. Rev. C **73**, 031301 (2006).

[28] J. C. Pei, F. R. Xu, Z. J. Lin, and E. G. Zhao, Phys. Rev. C **76**, 044326 (2007).

[29] Y. Qian, Z. Ren, and D. Ni, J. Phys. G: Nucl. Part. Phys. **38**, 015102 (2011).

[30] Y. Qian and Z. Ren, Phys. Rev. C **88**, 044329 (2013).

[31] D. Ni and Z. Ren, Phys. Rev. C **80**, 051303 (2009).

[32] M. Ismail, A. Y. Ellithi, M. M. Botros, and A. Adel, Phys. Rev. C **81**, 024602 (2010).

[33] W. M. Seif, M. Shalaby, and M. F. Alrakshy, Phys. Rev. C **84**, 064608 (2011).

[34] D. N. Poenaru, H. Stöcker, and R. A. Gherghescu, Eur. Phys. J. A **54**, 14 (2018).

[35] A. Parkhomenko and A. Sobiczewski, Acta Phys. Pol. B **36**, 1363 (2005).

[36] A. Sobiczewski and K. Pomorski, Prog. Part. Nucl. Phys. **58**, 292 (2007).

[37] D. N. Poenaru and W. Greiner, Phys. Scr. **44**, 427 (1991).

[38] D. N. Poenaru, R. A. Gherghescu, and W. Greiner, Phys. Rev. Lett. **107**, 062503 (2011).

[39] D. N. Poenaru, R. A. Gherghescu, and W. Greiner, Phys. Rev. C **85**, 034615 (2012).

[40] E. Hourani, M. Hussonnois, and D. N. Poenaru, Ann. Phys. Fr. **14**, 311 (1989).

[41] Y. Z. Wang, S. J. Wang, Z. Y. Hou, and J. Z. Gu, Phys. Rev. C **92**, 064301 (2015).

[42] V. E. Viola and G. T. Seaborg, J. Inorg. Nucl. Chem. **28**, 741 (1966).

[43] D. N. Poenaru, M. Ivascu, and D. Mazilu, Comput. Phys. Commun. **25**, 297 (1982).

[44] D. N. Poenaru, R. A. Gherghescu, and N. Carjan, Europhys. Lett. **77**, 62001 (2007).

[45] D. Ni, Z. Ren, T. Dong, and C. Xu, Phys. Rev. C **78**, 044310 (2008).

[46] D. N. Poenaru, I. H. Plonski, R. A. Gherghescu, and W. Greiner, J. Phys. G: Nucl. Part. Phys. **32**, 1223 (2006).
[47] D. N. Poenaru, R. A. Gherghescu, and W. Greiner, J. Phys. G: Nucl. Part. Phys. **39**, 015105 (2012); **40**, 105105 (2013).
[48] D. T. Akrawy and D. N. Poenaru, J. Phys. G: Nucl. Part. Phys. **44**, 105105 (2017).
[49] D. S. Delion and R. J. Liotta, Phys. Rev. C **87**, 041302 (2013).
[50] C. Qi, A. N. Andreyev, M. Huyse, R. J. Liotta, P. Van Duppen, and R. Wyss, Phys. Lett. B **734**, 203 (2014).
[51] D. S. Delion, A. Dumitrescu, and V. V. Baran, Phys. Rev. C **93**, 044321 (2016).
[52] C. Qi, A. N. Andreyev, M. Huyse, R. J. Liotta, P. Van Duppen, and R. A. Wyss, Phys. Rev. C **81**, 064319 (2010).
[53] Y. Ando and T. Itoh, J. Appl. Phys. **61**, 1497 (1987).
[54] Y. Qin, J. Tian, Y. Yang, and N. Wang, Phys. Rev. C **85**, 054623 (2012).
[55] P. Möller, A. J. Sierk, T. Ichikawa, and H. Sagawa, At. Data Nucl. Data Tables **109-110**, 1 (2016).
[56] G. Audi, F. G. Kondev, M. Wang, W. J. Huang, and S. Naimi, Chin. Phys. C **41**, 030001 (2017).
[57] M. Wang, G. Audi, F. G. Kondev, W. J. Huang, S. Naimi, and X. Xu, Chin. Phys. C **41**, 030003 (2017).
[58] NNDC of the Brookhaven National Laboratory, http://www.nndc.bnl.gov